NACA

RESEARCH MEMORANDUM

AERODYNAMICS OF MISSILES EMPLOYING WINGS OF VERY LOW ASPECT RATIO

By Elliott D. Katzen and Leland H. Jorgensen

Ames Aeronautical Laboratory
Moffett Field, Calif.

NATIONAL ADVISORY COMMITTEE FOR AERONAUTICS

WASHINGTON

March 5, 1956

NATIONAL ADVISORY COMMITTEE FOR AERONAUTICS

RESEARCH MEMORANDUM

AERODYNAMICS OF MISSILES EMPLOYING WINGS OF VERY LOW ASPECT RATIO

By Elliott D. Katzen and Leland H. Jorgensen

INTRODUCTION

Development tests such as those made by the Douglas and Hughes Aircraft Companies (e.g., refs. 1 to 5) have shown that, for certain applications, missiles employing wings of very low aspect ratio have excellent aerodynamic characteristics. Other studies have focused attention on low aspect ratios by questioning the need for wings of large span or even wings at all. There have been, however, large gaps in our knowledge concerning the aerodynamics of missiles having wings of very low aspect ratio. To help fill some of the gaps, wind-tunnel tests have been performed on a family of missiles. This paper summarizes the results of the investigation; some of the performance and stability and control characteristics of the missiles are discussed.

TESTS

The models studied are shown in figure 1. The basic body had a total fineness ratio of 10, being composed of a fineness-ratio-3 ogival nose and a cylindrical afterbody. In some instances the models were also tested with a Newtonian minimum-drag nose of fineness ratio 5; this resulted in a total fineness ratio of 12.

The aspect ratios of the wings were varied from a little less than 0.1 to 1. This corresponds, for the triangular wings, to semiapex angles from 1.3° to 14°. The wing sections were modified flat plates with leading and trailing edges generally beveled to small radii. In some cases the leading edges were not sharpened but were blunted with relatively large radii.

Various methods of controlling the models were studied. The tail control shown was tested in line and interdigitated 45° with respect to the wings. For comparison with the tail control, the nose of the model was deflected as a control. The planform area of this deflected portion of the nose was equal to that of 2 tail panels.

Data for these models were obtained at Mach numbers of 2.0, 2.9, and 3.3. The angle-of-attack range of the tests was from 0° to 30°; the control-deflection range was $\pm 45^{\circ}$. The Reynolds number was about 9×10^{6} based on the length of the basic body.

RESULTS AND DISCUSSION

Performance Characteristics

The lift of the missiles increases, of course, as planform area is added to the body. However, the question arises of whether the lift effectiveness, or lift per unit area, is also increased by the addition of very small wings. The lift effectiveness of winged and wingless missiles is compared in figure 2. The coefficients are based on total planform area; therefore they represent lift per unit area. At a lift ratio of unity, the lift per unit area is equal to that of the body. Above this value (represented by the dashed line), the lift per unit area is increased to more than that of the body. Even the smallest wing (aspect ratio of 3/32) increases the lift effectiveness appreciably to more than that of the body (fig. 2(a)). At a Mach number of 3.3 and an angle of attack of 10°, for example, the lift per unit area is increased 20 percent by the addition of this small wing. The total lift of this configuration, moreover, is increased an additional 10 percent; this additional increase results in a total increase of 30 percent, because the planform area is increased 10 percent over that of the basic body. As the Mach number or the angle of attack is increased, the lift effectiveness approaches that of the body more closely.

The data presented in figure 2(a) pertain to the family of missiles having wings whose root chords are the same length. As shown in figure 2(b), essentially the same results have been obtained at Mach number 3.3 for other missiles of constant span. It is interesting to note that the geometrically slender models cannot be considered aerodynamically slender at this high a Mach number. By slender-body theory, wing-body combinations of equal span have the same lift. Hence, the lift per unit area should decrease as additional wing area is added to the body. However, the lift of the combinations can be calculated with fair accuracy by the use of standard interference methods (e.g., ref. 6) which use slender-body theory only for the interference ratios. For missiles having very small wings it is especially important in these calculations that the lift of body alone be known accurately either from theory or experiment.

Other wind-tunnel data (ref. 7) for Mach numbers even as high as 6 show that lift effectiveness is much greater for winged than wingless

missiles. Depending on specific design considerations, the presence of even a very small wing could improve the lift and maneuverability of a missile over a wide range of Mach number and angle of attack. Of course, the increased weight due to the addition of wings has to be considered.

The increase in fore drag that results from adding wings to the basic body is indicated in figure 3. The drag coefficients are based on the cross-sectional area of the body rather than on total planform area as in figure 2. The drag decreased as the Mach number was increased from 2.0 to 2.9, but there was little difference between the data for Mach numbers 2.9 and 3.3. The horizontal bars in figure 3 indicate the relatively small spread in minimum drag coefficient for the missiles with leading edges curved in planform. These missiles all have the same planform area as the model having wings of aspect ratio 3/8 and straight leading edges. For this same missile, increasing the nose fineness ratio from 3 to 5 reduced the minimum drag coefficient about 30 percent. The effect of changing from a wing section with a relatively sharp leading edge to a section having a blunt leading edge was negligible for this model with aspect ratio 3/8. This indicates that large drag penalties will not be incurred by blunting the leading edges of these highly swept wings to alleviate aerodynamic heating.

In figure 4 the variation with planform area of another performance parameter, the maximum ratio of lift to drag, is illustrated. Increasing planform area (and aspect ratio) increased $(L/D)_{MAX}$, the variation being almost linear. The effect of an increase in Mach number from 2.0 to 3.3 is to cause a decrease in $(L/D)_{MAX}$ for the configurations having the largest wings. Here, wing characteristics are beginning to predominate; the decrease is due principally to the decrease in wing lift-curve slope and, therefore, increased drag due to lift with this increase in Mach number. Since skin-friction is a relatively large part of the drag of these configurations, it must be emphasized that these results were obtained at a Reynolds number of about 9×10^6. Therefore, care should be taken in applying these results to conditions at other Reynolds numbers. The angle of attack for $(L/D)_{MAX}$ decreased from about 11° for the body alone to 6° for the missile having the largest wing. Increasing the nose fineness ratio from 3 to 5 increased $(L/D)_{MAX}$ by about 20 percent. Further increases in $(L/D)_{MAX}$ could be made by taking advantage of some of the favorable interference effects discussed in reference 8.

Stability and Control Characteristics

Performancewise, the advantages of missiles having low-aspect-ratio wings have been discussed. Now the stability and control characteristics of these same models will be presented. In figure 5, the center of pressure, in diameters from the nose, is plotted as a function of angle of attack. The curve for the body alone shows that the center of pressure starts out near the nose at zero angle of attack and moves toward the body centroid of area as the angle of attack is increased. The center-of-pressure position of the body alone can be predicted within less than half a diameter. Adding even a very small wing significantly reduces the center-of-pressure travel with changes in angle of attack and moves the center of pressure rearward, thereby resulting in a more stable configuration. The center of pressure continues to move rearward as the wing aspect ratio is increased and additional wing area is added to the missile. The center-of-pressure travel with angle of attack was negligible for the missiles having wings of aspect ratios 3/8, 2/3, and 1 at this Mach number of 3.3.

The effect of Mach number changes on center of pressure is shown in figure 6. The center-of-pressure movement with changes in Mach number was large for the body alone and decreased as the wing aspect ratios were increased from 0 to 3/8. For the missile having a wing of aspect ratio 3/8, the center-of-pressure travel with changes in Mach number and angle of attack was less than 0.4d. The travel was slightly larger for the configurations with wings of aspect ratios 2/3 and 1. Changes in bank angle of the missiles also caused shifts in center of pressure. The shifts were negligible for the missiles with the smallest wings. For the missile having the largest wing, the effect of changes in bank angle was to approximately double the center-of-pressure travel with changes in angle of attack and Mach number. Results from Douglas Aircraft Co., Inc. (ref. 1) have shown that the already small center-of-pressure shifts associated with configurations like these can be further reduced by the use of small fixed surfaces forward of the wing. These canard surfaces do increase the rolling moments, however, at high angles of attack.

In addition to making the center-of-pressure shifts small, it is desirable to be able to fix the center of pressure at certain positions along the body length. A method of accomplishing this is shown in figure 7. The center of pressure of missiles having wing leading edges curved in planform are shown. The curved leading edges change the centroid of area. For comparison (with the curved-leading-edge data), data for the body alone and for the configuration having a straight-leading-edge wing of aspect ratio 3/8 are repeated from figure 6. The center-of-pressure positions are consistent with the changes in the centroid of planform area. The center of pressure of the model with a convex leading edge was farther forward and the center of pressure of the model with a

concave leading edge was farther aft than that for the missile having a wing with a straight leading edge. The configuration having the small wing extending to the tip of the nose was much more stable than the body alone but less stable than the other configurations. The small center-of-pressure shifts associated with these configurations having wings of very low aspect ratio simplify the problem of stabilizing and controlling the missiles.

The effect on missile stability of three types of controls, in-line and interdigitated tail controls and swivel nose, is illustrated in figure 8. The tail controls are composed of single-wedge sections to increase their effectiveness and reduce control center-of-pressure travel with changes in Mach number, thereby reducing hinge moments. The controls are small enough so that their blunt trailing edges do not appreciably increase missile drag. The diamond planform was chosen to reduce control center-of-pressure travel with changes in Mach number. Another reason for this choice is that the diamond planform is structurally adaptable to interdigitation; the control need not be attached to the wing as a short-chord high-aspect-ratio control would. For the examples shown in figure 8, the controls were placed on the missile having a straight-leading-edge wing of aspect ratio 3/8. The pitching-moment coefficients presented are based on body diameter and cross-sectional area. The center-of-gravity location (0.60L, 0.59L, and 0.58L for the interdigitated tail, in-line tail, and swivel-nose models) was chosen so that the three configurations had the same static margin with 0° control deflection at low normal-force coefficients at a Mach number of 2.0. At this Mach number the nose control has the least effectiveness. The effectiveness of the in-line tail control is greater than that of the nose control. The interdigitated control, by virtue of being removed from the wing wake, has greater effectiveness than the in-line control. Control deflections of 15° are adequate for the interdigitated control for obtaining high values of trim normal force.

In figure 9 the effect of control type on stability is again illustrated, but at $M = 3.3$. The center-of-gravity positions have not been changed from those chosen for the data at $M = 2.0$. With the increase in Mach number the effectiveness of the swivel nose has increased so that it now has approximately the same effectiveness as the interdigitated control. The effectiveness of the two tail controls has decreased appreciably.

In figure 10 the effect of planform on missile stability is presented. The same interdigitated tail control was placed on 3 missiles having wings differing in size and aspect ratio. The data were obtained at Mach number 3.3. Here, again, the center of gravity (0.48L, 0.60L, and 0.62L for the models having wings of aspect ratio 3/32, 3/8, and 1) was chosen so that the different missiles have the same static margin for small normal-force coefficients and 0° control deflection. For

15° control deflection the control effectiveness is adequate at low normal-force coefficients for the missile having the smallest wing. However, large trim normal-force coefficients were not obtained because of the relatively large center-of-pressure travel associated with this configuration. The effectiveness is naturally low for the missile having the largest wing because the control is small relative to the wing size. On the other hand, the effectiveness of the control on the missile having a wing of aspect ratio 3/8 is sufficient to trim the missile to large normal-force coefficients.

In figure 11 the effect of various arrangements on rolling moment is illustrated. Rolling-moment coefficient, based on exposed wing area and total span, is plotted as a function of resultant angle of attack. The data are presented for bank angles of 22.5° for cruciform and 45° for monowing models, since maximum rolling moments occur close to these bank angles. The rolling moments are considerably larger for the monowing than for the cruciform arrangement of the same model. The effect of increased forebody length, for the model having this same wing of aspect ratio 3/8, can also be seen to increase the rolling moments. This increase is indicated qualitatively, as discussed in reference 9, by calculations that account for the increased vortex strength associated with the increased forebody length. It is interesting to note that the rolling-moment coefficients fall on the same curve for the cruciform models having the same nose length but wing aspect ratios of 3/8 and 1. The magnitude of the rolling moments for all configurations was less than the amount that was obtained by differential deflection of the interdigitated tail control.

CONCLUDING REMARKS

The results of this investigation indicate that there are distinct aerodynamic advantages to the use of wings of very low aspect ratio for missiles. Some of these advantages performancewise are high lift, compared to wingless missiles, and low drag with shapes that appear to be beneficial for combatting aerodynamic heating. From the standpoint of stability and control, these missiles exhibit small center-of-pressure shifts and small rolling moments for a wide range of supersonic Mach numbers and combined angles of attack and bank so that control problems are simplified.

Ames Aeronautical Laboratory
National Advisory Committee for Aeronautics
Moffett Field, Calif., Nov. 2, 1955

REFERENCES

1. Buquoi, T. W.: Presentation of Force and Moment Data From a Wind Tunnel Test of an 0.0333 Scale Wing Planform Development Model for the 1810 Missile at Mach Numbers 1.61, 1.97, 2.54, and 2.80 (Phases II and III). Rep. No. SM-18420 (Contract No. DA-30-069-ORD-1082), Douglas Aircraft Co., Inc., Aug. 23, 1954.

2. Buquoi, T. W.: Presentation of Force and Moment Data From Wind Tunnel Tests of an 0.6 Scale Control Development Model for the 1810 Missile at Mach Numbers 1.97, 2.55, and 3.67. Rep. No. SM-14929 (Contract No. DA-30-069-ORD-1082), Douglas Aircraft Co., Inc., Apr. 12, 1954.

3. Edgar, J. M.: Presentation of Force and Moment Data from a Supersonic Wind-Tunnel Test of a 0.06 Scale Hinge Moment Model with Plain-Balanced Elevons for the Model 1810 Missile. Rep. No. SM-18787, Douglas Aircraft Co., Inc., Mar. 2, 1955.

4. Buquoi, T. W.: Presentation of Force and Moment Data From a Wind Tunnel Test of an 0.0333 Scale Wing Planform Development Model for the 1810 Missile at Mach Numbers 1.61, 1.97, 2.54, and 2.80 (Phase I). Rep. No. SM-18410 (Contract No. DA-30-069-ORD-1082), Douglas Aircraft Co., Inc., Aug. 23, 1954.

5. Marriott, Edwin O.: Wind Tunnel Tests of Various Balanced Control Surfaces at Mach Numbers From 1.33 to 4.50. Hughes Aircraft Co. Res. and Dev. Labs. (Culver City, Calif.), Sept. 10, 1952.

6. Nielsen, Jack N., Kaattari, George E., and Anastasio, Robert F.: A Method for Calculating the Lift and Center of Pressure of Wing-Body-Tail Combinations at Subsonic, Transonic, and Supersonic Speeds. NACA RM A53G08, 1953.

7. Neice, Stanford E., Wong, Thomas J., and Hermach, Charles A.: Lift, Drag, and Static Longitudinal Stability Characteristics of Four Airplane-Like Configurations at Mach Numbers From 3.00 to 6.28. NACA RM A55C24, 1955.

8. Rossow, Vernon J.: A Theoretical Study of the Lifting Efficiency at Supersonic Speeds of Several Airfoil and Fuselage Combinations Which Utilize Indirect Lift. NACA RM A55L08, 1956.

9. Nielsen, Jack N., Spahr, J. Richard, and Centolanzi, Frank: Aerodynamics of Bodies, Wings, and Wing-Body Combinations at High Angles of Attack and Supersonic Speeds. NACA RM A55L13c, 1956.

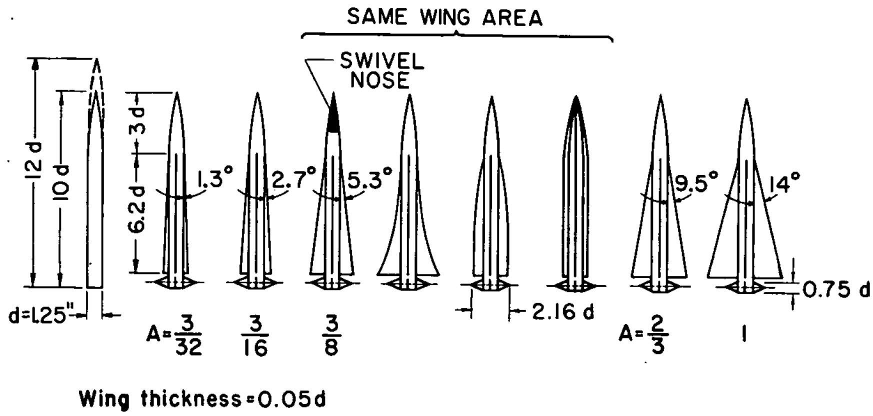

Figure 1

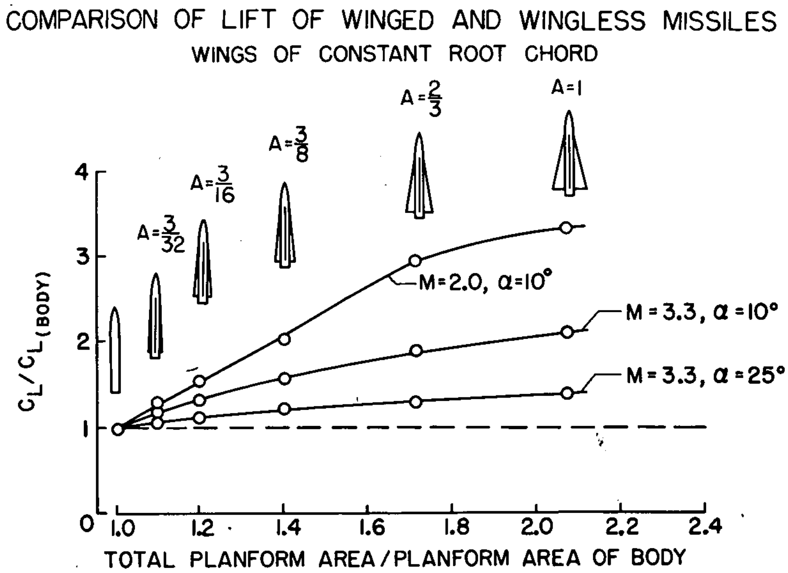

Figure 2(a)

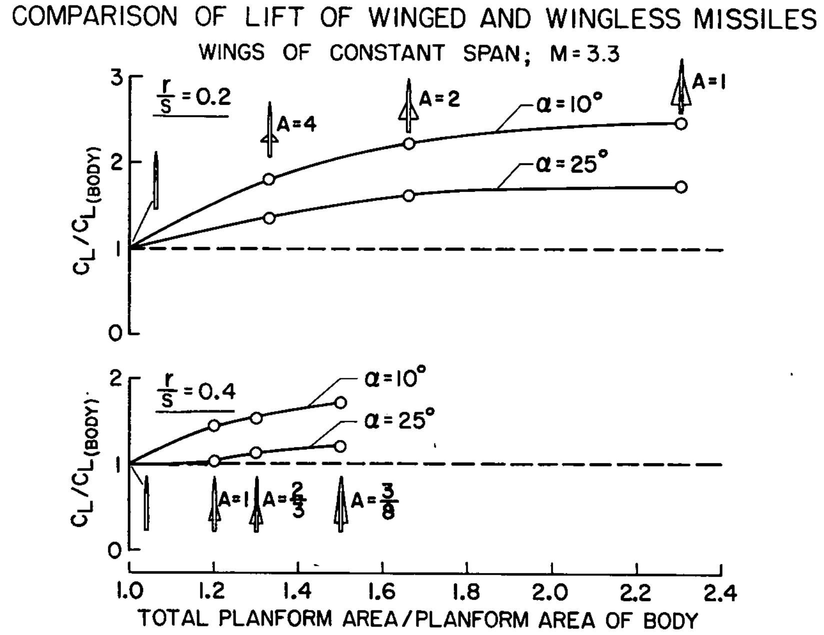

Figure 2(b)

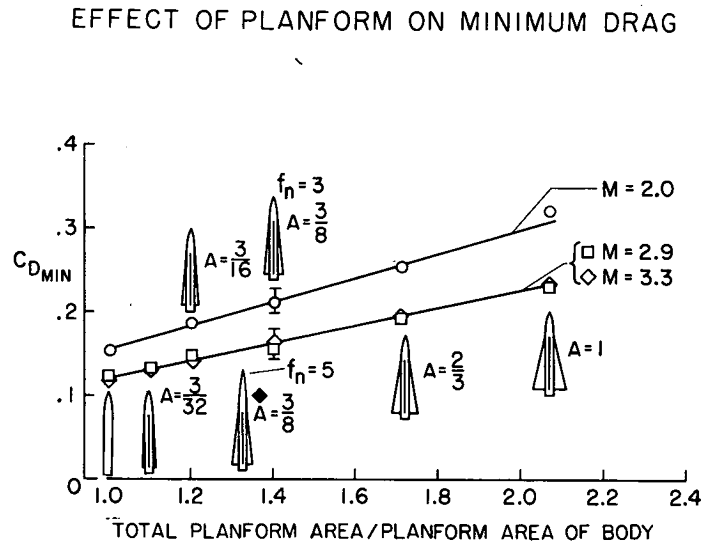

Figure 3

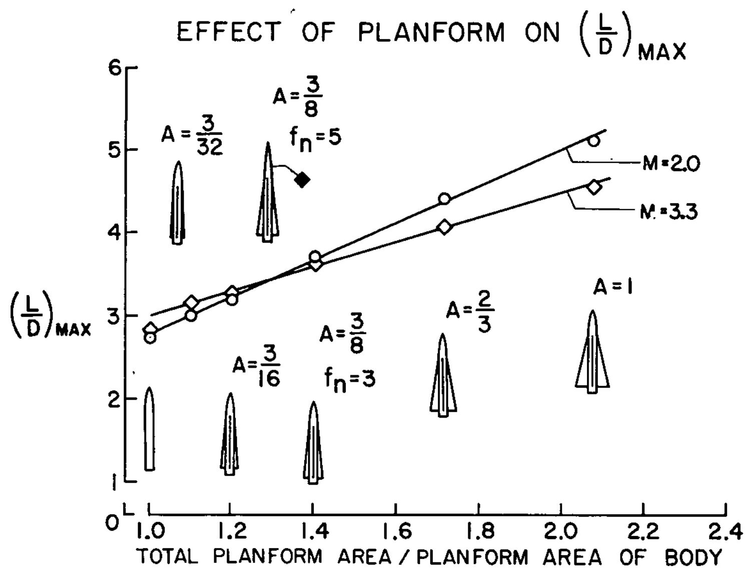

Figure 4

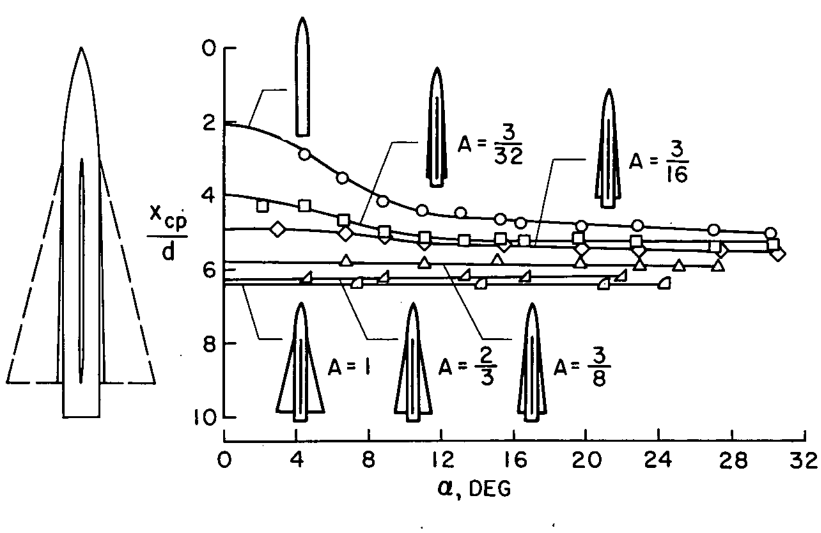

Figure 5

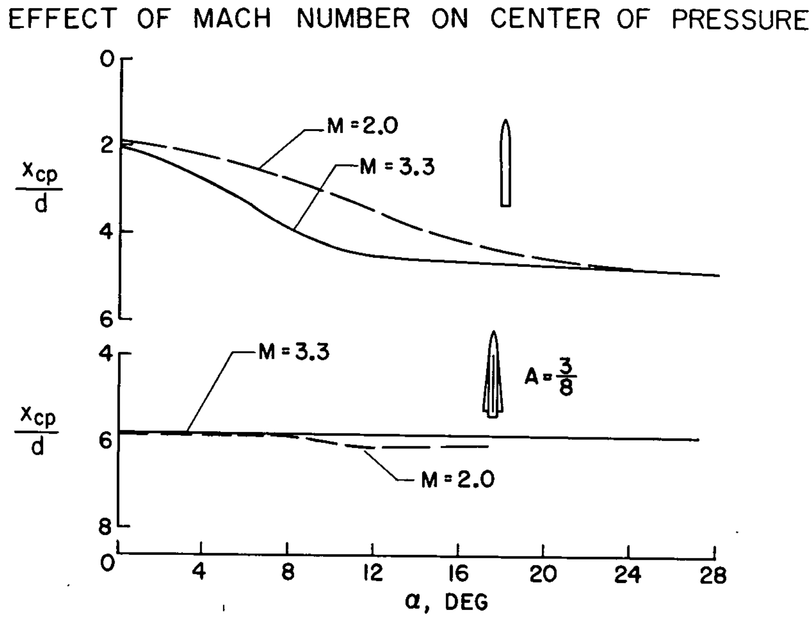

Figure 6

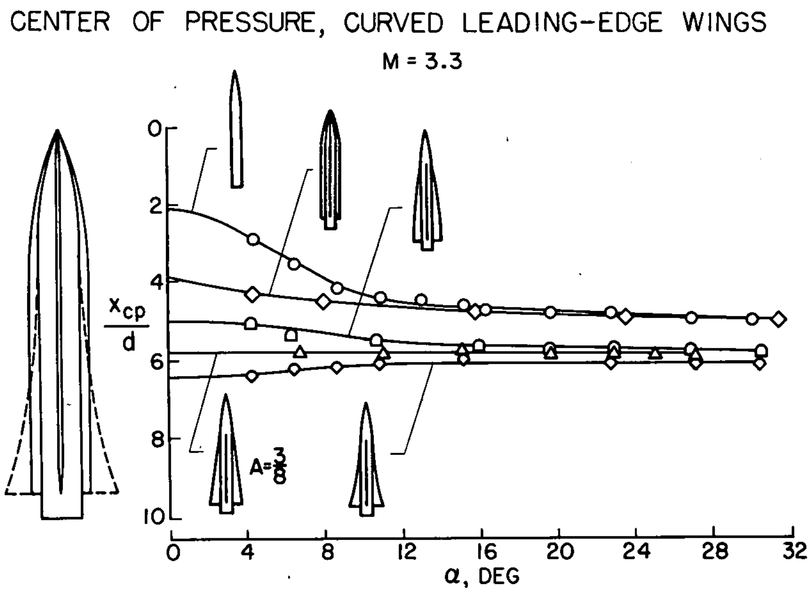

Figure 7

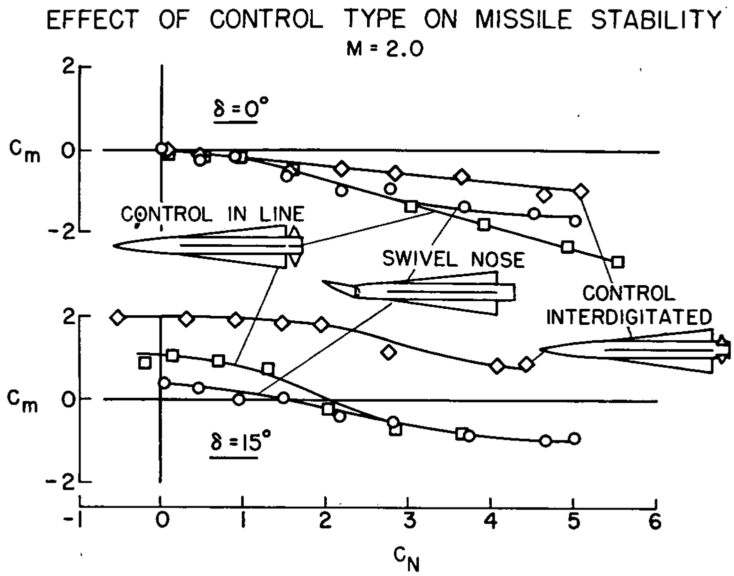

Figure 8

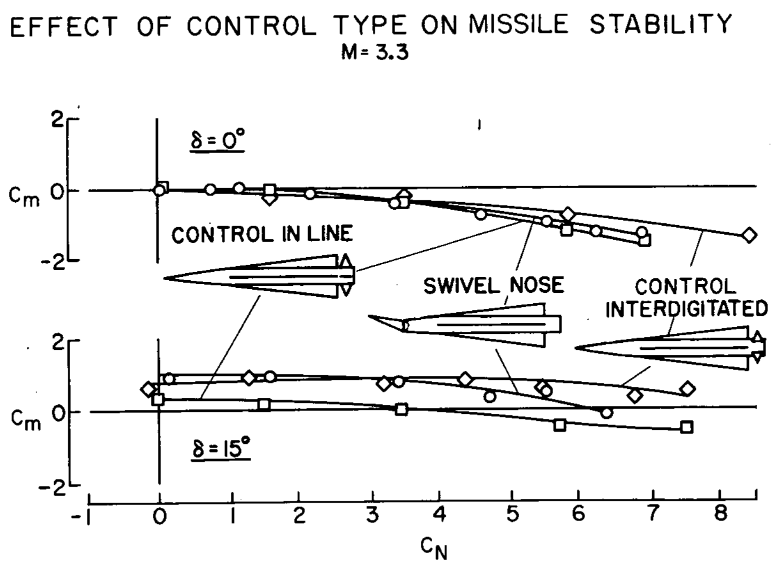

Figure 9

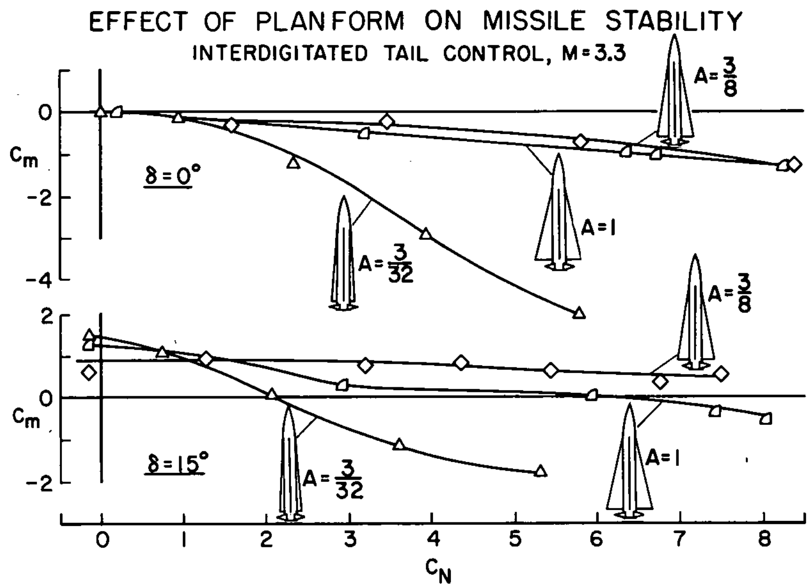

Figure 10

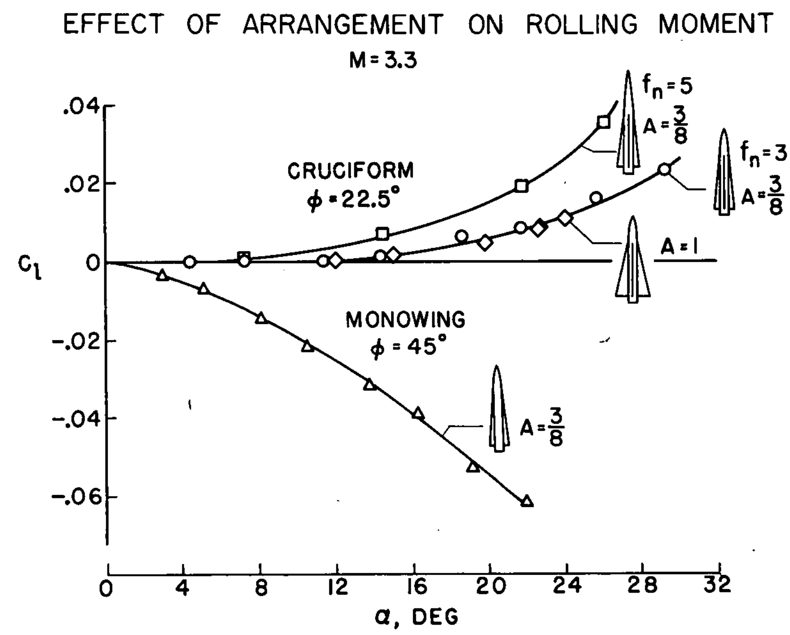

Figure 11

NACA - Langley Field, Va.

UNCLASSIFIED